THE JOURNAL OF BIOLOGICAL CHEMISTRY VOL. 284, NO. 18, pp. 12165–12177, May 1, 2009

Cross-talk between Type Three Secretion System and Metabolism in *Yersinia*[*] [S]

Received for publication, February 3, 2009, and in revised form, February 24, 2009 Published, JBC Papers in Press, February 25, 2009, DOI 10.1074/jbc.M900773200

Annika Schmid[‡1], Wibke Neumayer[‡1], Konrad Trülzsch[‡], Lars Israel[§], Axel Imhof[§], Manfred Roessle[¶], Guido Sauer[‖], Susanna Richter[‡], Susan Lauw[‡‡], Eva Eylert[‡‡], Wolfgang Eisenreich[‡‡], Jürgen Heesemann[‡], and Gottfried Wilharm[‡§§2]**

*From the [‡]Department of Bacteriology, Max von Pettenkofer-Institute for Hygiene and Medical Microbiology, Pettenkoferstrasse 9a, D-80336 Munich, the [§]Adolf-Butenandt-Institute, Schillerstrasse 44, D-80336 Munich, the [¶]European Molecular Biology Laboratory, Hamburg Outstation, c/o Deutsches Elektronen-Synchrotron, Notkestrasse 85, D-22603 Hamburg, the [‖]Institute of Clinical Molecular Biology and Tumor Genetics, Forschungszentrum für Umwelt und Gesundheit-National Research Center for Environment and Health, Marchioninistrasse 25, D-81377 Munich, the **Max Planck Institute for Developmental Biology, Spemannstrasse 35/II, D-72076 Tübingen, the [‡‡]Lehrstuhl für Biochemie, Department Chemie, Technische Universität München, Lichtenbergstrasse 4, D-85747 Garching, and the [§§]Robert Koch-Institute, Wernigerode Branch, Burgstrasse 37, D-38855 Wernigerode, Germany*

Pathogenic yersiniae utilize a type three secretion system (T3SS) to inject Yop proteins into host cells in order to undermine their immune response. YscM1 and YscM2 proteins have been reported to be functionally equivalent regulators of the T3SS in *Yersinia enterocolitica*. Here, we show by affinity purification, native gel electrophoresis and small angle x-ray scattering that both YscM1 and YscM2 bind to phosphoenolpyruvate carboxylase (PEPC) of *Y. enterocolitica*. Under *in vitro* conditions, YscM1, but not YscM2, was found to inhibit PEPC with an apparent IC_{50} of 4 μM (K_i = 1 μM). To analyze the functional roles of PEPC, YscM1, and YscM2 in Yop-producing bacteria, cultures of *Y. enterocolitica* wild type and mutants defective in the formation of PEPC, YscM1, or YscM2, respectively, were grown under low calcium conditions in the presence of [U-$^{13}C_6$]glucose. The isotope compositions of secreted Yop proteins and nine amino acids from cellular proteins were analyzed by mass spectrometry. The data indicate that a considerable fraction of oxaloacetate used as precursor for amino acids was derived from [$^{13}C_3$]phosphoenolpyruvate by the catalytic action of PEPC in the wild-type strain but not in the PEPC$^-$ mutant. The data imply that PEPC is critically involved in replenishing the oxaloacetate pool in the citrate cycle under virulence conditions. In the YscM1$^-$ and YscM2$^-$ mutants, increased rates of pyruvate formation via glycolysis or the Entner-Doudoroff pathway, of oxaloacetate formation via the citrate cycle, and of amino acid biosynthesis suggest that both regulators trigger the central metabolism of *Y. enterocolitica*. We propose a "load-and-shoot cycle" model to account for the cross-talk between T3SS and metabolism in pathogenic yersiniae.

Type three secretion systems (T3SSs)[3] are used by several Gram-negative bacteria as microinjection devices to deliver effector proteins into host cells (1). The translocated effector proteins reprogram the host cell in favor of the microbial invader or symbiont. Pathogenic yersiniae (the enteropathogenic *Yersinia enterocolitica* and *Yersinia pseudotuberculosis* and the plague bacillus *Yersinia pestis*) utilize a plasmid-encoded T3SS to undermine the host primary immune response (2). This is mediated by the injection of a set of effector proteins called Yops (*Yersinia* outer proteins) into host cells, in particular into cells with innate immune functions, such as macrophages, dendritic cells, and neutrophils (3). The concerted action of Yops, targeting multiple signaling pathways, results in actin cytoskeleton disruption, suppression of proinflammatory signaling, and induction of apoptosis. This strategy enables yersiniae to multiply extracellularly in host tissue.

Expression of the *Yersinia* T3SS is up-regulated at 37 °C, and translocation of Yops across the host cell membrane is triggered by cell contact (4, 5). Pathogenic yersiniae cultivated under low calcium conditions at 37 °C express a phenotype referred to as "low calcium response" (LCR). The LCR is characterized by growth restriction as well as massive expression and secretion of Yops into the culture medium (6–9). The allocation of energy and metabolites for the massive synthesis and transport of Yops is demanding, and this burden is believed to be responsible for the observed growth inhibition (10). To give an idea of the metabolic requirements, Yops are secreted to the culture supernatant in 10-mg amounts per liter of culture within 2 h after calcium depletion of the medium. Furthermore, post-translationally secreted substrates need to be unfolded by a T3SS-specific ATPase prior to secretion (11–14). In addition, T3SS-dependent transport of Yops requires the proton motive force (15). However, there is evidence that growth cessation and Yop expression can be uncoupled (16, 17), suggesting a coordinated regulation of metabolism and protein transport rather than the LCR reflecting an inevitable physiological consequence.

What are the candidate proteins that could be involved in such a coordination? YscM1 and YscM2 (57% identical to YscM1) are key candidates, since they act at a major nodal point

* This work was supported by Deutsche Forschungsgemeinschaft Grants SFB 594, Teilprojekt B6, GRK 303, and SPP 1316.
[S] The on-line version of this article (available at http://www.jbc.org) contains supplemental Tables S1–S3 and Figs. S1–S7.
[1] Both of these authors contributed equally to this work.
[2] To whom correspondence should be addressed: Robert Koch-Institut, Bereich Wernigerode, Burgstr. 37, D-38855 Wernigerode, Germany. Tel.: 49-3943-679-282; Fax: 49-3943-679-207; E-mail: wilharmg@rki.de.
[3] The abbreviations used are: T3SS, type III secretion system; LCR, low calcium response; PEPC, phosphoenolpyruvate carboxylase; PEP, phosphoenolpyruvate; GST, glutathione *S*-transferase; SAXS, small angle x-ray scattering; MALDI, matrix-assisted laser desorption ionization; TOF, time-of-flight; BHI, brain heart infusion; GC, gas chromatography; MS, mass spectrometry.

of the T3SS regulatory network in *Y. enterocolitica*. In *Y. pestis* and *Y. pseudotuberculosis*, only the YscM1 homologue LcrQ exists (99% identical to YscM1). YscM1/LcrQ and YscM2 are secretion substrates of the T3SS that are involved in up-regulation of Yop expression after host cell contact. Upon cell contact, the decrease of intracellular levels of YscM1/LcrQ and YscM2 due to their translocation into host cells results in a derepression of Yop synthesis (18–21). The two *yscM* copies of *Y. enterocolitica* were presumed to be functionally equivalent, since deletion of either gene was found to be phenotypically silent (19, 22). Only deletion of both *yscM* genes could establish the *lcrQ* phenotype (19, 22), distinguished by temperature sensitivity for growth, derepressed Yop expression, and secretion of LcrV and YopD in the presence of calcium ions.

YscM1/LcrQ as well as YscM2 exhibit homology to the N terminus of the effector YopH (19, 23, 24), a fact that may explain their shared assistance by SycH (specific Yop chaperone) (20, 25). It was shown that YscM1/LcrQ and YscM2 exert their influence on Yop expression in concert with the T3SS components SycH, SycD (LcrH in *Y. pestis* and *Y. pseudotuberculosis*), and YopD (21, 26–28). It is further described that YscM1 and/or YscM2 interact with several of the T3SS-specific chaperones, in particular with SycH, SycE, SycD, and SycO (20, 29–31). This has led to the model that YscM/LcrQ proteins might function as an interface that senses whether chaperones are loaded with Yops and transduces these signals into control of Yop expression (14).

These features of YscM1/LcrQ and YscM2 prompted us to speculate about a key role of these proteins in coordination of metabolism and expression of T3SS components. Using recombinant GST-YscM1 and GST-YscM2 as bait for *Y. enterocolitica* cytosolic proteins, we identified phosphoenolpyruvate carboxylase (PEPC) as interaction partner of both YscM1 and YscM2. Under *in vitro* conditions, YscM1 down-regulated PEPC activity and bacterial growth/replication. Isotopologue profiling of Yop proteins and derived amino acids from *Y. enterocolitica* grown in the presence of [U-$^{13}C_6$]glucose showed the functionality of the PEPC reaction under virulence conditions (isotopologues are molecular entities that differ only in isotopic composition (number of isotopic substitutions); *e.g.* CH_4, CH_3D, and CH_2D_2). Moreover, biosynthetic rates of amino acids were increased in mutants defective in YscM1 or YscM2, suggesting a general role of these regulators in the metabolism of *Y. enterocolitica*. Recently, evidence has been accumulating that the metabolic state contributes to the regulation of T3SSs of diverse pathogens, also including the flagellar T3SS in *Pseudomonas* and *Salmonella* (32–36).

EXPERIMENTAL PROCEDURES

Cloning and Mutagenesis—For details on construction of plasmids and mutants, see below. Overproduction of YscM1 and YscM2 was based on plasmid pWS (37) and controlled by an isopropyl β-D-thiogalactoside-inducible *tac* promoter. For purification of recombinant *Yersinia* PEPC, a GST fusion construct based on pGEX-4T3 (Amersham Biosciences) was used. Plasmids for expression of GST-YscM1 and GST-YscM2 fusions have been described (38). The *ppc* mutant was generated as described (15) by replacement of the *ppc* gene with a kanamycin resistance cassette mediated by homologous recombination of a transformed PCR product. The primers used were 5′-CTAACAACCCTGCGGCGTCAAGGGCGAAGGGGATATGGGTCAGGGGTCATTCACTGACACCCTCATCAGTG-3′ and 5′-ACGGGCGCCTGGCCCGTTTTGTCTTTTATTCACGATAATTCTACTGGCAACGTCAAGTCAGCGTAATGCTC-3′. Construction of *yscM1* and *yscM2* deletion strains was previously described (31). After cleavage of pWS with NdeI and SalI, appropriate inserts with PCR-introduced NdeI and SalI sites, respectively, were ligated. As template, DNA from *Y. enterocolitica* WA-314 was used. For construction of pWS-YscM1 primers, 5′-CATATGAAAATCAATACTCTTCAATCG-3′ and 5′-GTCGACTCAGCCGTCAGCCG-3′ were used; for pWS-YscM2 construction, primers 5′-CATATGGGGAGCATTATGAAAAATAAACG-3′ and 5′-GTCGACTTAAAGCTTTTGCATTTTCCGTGTC-3′ were used. Primer design for YscM1 and YscM2 constructs was based on sequences with accession number AY150843.

Y. enterocolitica ppc was amplified by PCR with primers 5′-GAATTCAATGAACGAACAATATTCCGCAATGC-3′ and 5′-GCGGCCGCTTAGCCGGTATTACGCATACCTG-3′ introducing EcoRI and NotI restriction sites, and the *ppc* fragment was ligated into EcoRI-NotI-digested vector pGEX-4T3.

Protein Expression and Purification—YscM1 and YscM2 were fused to GST based on two vectors, pGEX-4T3 and pGEX-6P3 (Amersham Biosciences). GST fusions based on pGEX-4T3, which harbor a thrombin cleavage site, were used for initial PEPC binding studies (affinity purification and native gel electrophoresis). For production of recombinant YscM1/YscM2 without GST, pGEX-4T3-based constructs cannot be used, since YscM1/YscM2 harbor an intrinsic thrombin cleavage site (38). Therefore, recombinant YscM1 and YscM2 were produced as described using pGEX-6P3 as vector (38). Note, however, that GST-YscM1 and GST-YscM2 based on pGEX-6P3 were found to be incompetent to bind PEPC.

GST-PEPC was overproduced from plasmid pGEX-4T3-YePEPC in BL21 (DE3) pLysS (Stratagene) at 27 °C after the addition of 0.2 mM isopropyl β-D-thiogalactoside at an A_{600} of ~0.8. Bacterial pellets were harvested after cultivation overnight and subsequently frozen. Cells were lysed in 50 mM Tris-HCl, pH 7.5, 100 mM NaCl, 5 mM dithiothreitol. GST-PEPC was bound to GSH-Sepharose 4 FF and cleaved on site with thrombin. PEPC washed from the matrix after cleavage was subjected to gel filtration on a Superdex 200 (26/60) column equilibrated to 10 mM Tris-HCl, pH 8.0, 100 mM NaCl, 1 mM dithiothreitol. GST was expressed from plasmid pGEX-4T3 and purified according to the manufacturer's recommendations (Amersham Biosciences).

Affinity Purification and Identification of PEPC—Glutathione-Sepharose beads preloaded with GST fusions or GST as a control were incubated with lysates of *Y. enterocolitica* cells (WA-314, harboring the virulence plasmid pYV, and WA-C, a WA-314 derivative cured of pYV). Yersiniae were therefore cultured in brain heart infusion (BHI) medium at 27 °C (no expression of the pYV-encoded T3SS) and in parallel at 37 °C in the presence of 5 mM EGTA and 10 mM $MgCl_2$ (expression and secretion of Yops). Harvested cells were resuspended in PBS and disrupted by French press treatment. Soluble fractions

after centrifugation (20,000 × *g*, 30 min, 4 °C) were incubated with beads preloaded as described above at 4 °C for 1 h, and then beads were washed twice with phosphate-buffered saline and subjected to SDS-PAGE analysis. Coomassie-stained bands of interest were excised from the gel. Matrix-assisted laser desorption ionization-time of flight (MALDI-TOF) mass spectrometry (Reflex III; Bruker Daltonics GmbH, Bremen, Germany) was conducted as described recently (39) to identify PEPC as the ligand interacting with GST-YscM1 and GST-YscM2.

Native Gel Electrophoresis—Native gel electrophoresis was performed as described (40).

PEPC Activity Assay—PEPC activity was measured in a coupled reaction with malate dehydrogenase, as reported earlier (41). Assay components were 100 mM Tris-HCl, pH 8.0, 10 mM $NaHCO_3$, 10 mM $MgCl_2$, 0.2 mM NADH, 5 mM PEP, 1 unit of malate dehydrogenase, and 5 milliunits of PEPC. The reaction was initialized by the addition of PEP, and assay mixtures were incubated at 27 °C. The decrease of NADH absorption was monitored at 340 nm in a 96-well Nunc plate using a microplate reader (Biomolecular Devices; SpectraMax software). ΔA_{340} was determined by linear regression (typically, the correlation coefficient was 0.98 or above). We ruled out an effect of YscM1 on activity of malate dehydrogenase in the coupled reaction.

Growth under PEPC-requiring Conditions—Yersiniae (*Y. enterocolitica* WA-314) harboring plasmids pWS-YscM1, pWS-YscM2, and pWS were grown in rich medium overnight (BHI medium supplemented with 1% glucose) 1 day after selection of transformants. The next day, bacteria were pelleted, washed, and resuspended in M9 minimal salts supplemented with 1% glucose, 0.01% casamino acids, and 10 μg/ml thiamine. Under these conditions, the *ppc* mutant was unable to grow. 1 mM isopropyl β-D-thiogalactoside was added to all cultures at time 0 to induce overproduction of YscM1/YscM2 or as a control (WA-314 pWS). All experiments were performed in triplicate from independent cultures. Growth curves were determined by measuring optical density at 600 nm. Expression of the respective protein was controlled by Western blotting using polyclonal antiserum. It appeared crucial that these growth studies were performed the day after selection of transformants and that catabolite repression was maintained by the addition of glucose to selection plates and to overnight cultures to repress the *tac* promoter at best. Later analyses frequently resulted in a loss of YscM1 and YscM2 expression, suggesting a strong selection pressure of protein production.

^{13}C Labeling and Mass Spectrometry Analysis of Secreted Yops—Yersinae overnight cultures grown at 27 °C in BHI medium were centrifuged, and the pellet was washed twice in F-12 cell culture medium (Invitrogen; composition given in Table S1). Pellets were resuspended in F-12 medium, and suspensions were adjusted to an optical density (600 nm) of 0.15. F-12 medium was then supplemented with 2% [U-$^{13}C_6$]glucose or alternatively with 2% unlabeled glucose. To initially suppress secretion of Yops, the medium was supplemented with 0.2 mM $CaCl_2$. Cultures (3 ml) were grown for 2 h at 37 °C to stimulate expression of the T3SS, and then cultures were stimulated to secrete Yops by the addition of 5 mM EGTA and 10 mM $MgCl_2$. After 2 h of additional incubation at 37 °C, supernatants were collected by centrifugation, and the secreted proteins were precipitated with 10% tricarboxylic acid. Following separation on denaturing SDS gels, the Coomassie-stained protein bands corresponding to YopM, YopE, and YopH were excised from the gel, and the proteins were subjected to in-gel tryptic digestion and analyzed by MALDI-TOF mass spectrometry. To this end, Coomassie-stained protein bands from SDS gels were washed twice with water and twice with 40 mM NH_4HCO_3 buffer, pH 8.0. After 2-fold treatment with 50% acetonitrile for 5 min, trypsin (sequencing grade modified; Promega) was added, and proteins were digested overnight in 40 mM NH_4HCO_3 buffer, pH 8.0, at 37 °C while shaking. Probes were directly used for MALDI-TOF experiments. 10 μl of each sample were first purified and concentrated on a C18 reversed phase pipette tip (ZipTip; Millipore). The peptides were eluted with 1 μl of α-cyano-4-hydroxycinnamic acid (Sigma) and then directly spotted on a MALDI sample plate (Applied Biosystems). MALDI-TOF measurements were performed on a Voyager-DE STR TOF mass spectrometer (Applied Biosystems). The resulting spectra where displayed using the Data Explorer Software (Applied Biosystems).

When we became aware of the seemingly strong selection pressure relating to the YscM1 and YscM2 expression constructs (see above), we reasoned that the *yscM1* and *yscM2* deletion mutants may rapidly change genetically. On that account, we isolated the virulence plasmid of the *yscM1* and *yscM2* mutant, respectively, and transformed it into the plasmid-cured derivative WA-C of the parental strain WA-314, as recently described for Yop mutants (42).

^{13}C Labeling and Gas Chromatography-Mass Spectrometry Analysis of the Protein-derived Amino Acids—Yersinae cultures (200 ml) grown at 27 °C in BHI medium overnight were centrifuged, and the pellet was washed twice in F-12 cell culture medium (Invitrogen). Pellets were resuspended in F-12 medium, and 5-liter suspensions were adjusted to an optical density (600 nm) of 0.15. F-12 medium was supplemented with 0.2% [U-$^{13}C_6$]glucose or alternatively with 0.2% unlabeled glucose. The medium was supplemented with 0.2 mM $CaCl_2$ to suppress secretion of Yops initially. 5-liter cultures were grown in a pH-controlled BIOSTAT B fermenter for 2 h at 37 °C, and then cultures were stimulated to secrete Yops by the addition of 5 mM EGTA and 10 mM $MgCl_2$. After 2 h of additional incubation at 37 °C, bacterial cells were collected by centrifugation, frozen, and lyophilized. For gas chromatography/mass spectrometry (GC/MS) analysis, 5 mg of bacterial cell mass were hydrolyzed in 6 M HCl. The hydrolysate was dried and treated with *N*-(*tert*-butyldimethylsilyl)-*N*-methyl-trifluoroacetamide containing 1% *tert*-butyldimethylsilylchloride. The resulting *tert*-butyldimethylsilyl derivatives of amino acids were subjected to GC/MS, as described earlier (43). Samples were analyzed at least three times. Data were processed as described before (44), affording the molar excess of carbon isotopomer groups ($M + 1, M + 2, \ldots M + n$, with M being the mass ion of the fragment under study and n being the number of carbon atoms of the respective fragment). The excess of multiple labeled isotopologues was calculated according to the equation, $(2 \times (M + 2) + 3 \times (M + 3) + \ldots + n \times (M + n))/n$.

Small Angle X-ray Scattering Experiments and Data Analysis—The synchrotron radiation x-ray scattering data of PEPC alone, PEPC in complex with YscM1, and PEPC in complex with YscM2 were collected following standard procedures on the small angle scattering beamline X33 (45) of the EMBL Hamburg on the storage ring DORIS III of the Deutsches Elektronen Synchrotron. Details of data recording and processing are described in the supplemental material. The PEPC scattering was recorded at 2.4 mg/ml. PEPC-YscM1 and PEPC-YscM2 complexes were measured at a PEPC concentration of 0.6 and 1.6 mg/ml of the respective YscM protein. Protein solutions were equilibrated to phosphate-buffered saline using PD-10 cartridges for buffer exchange (GE Healthcare).

RESULTS

YscM1 and YscM2 Interact with PEPC—In order to identify interaction partners of YscM1 and YscM2, we incubated glutathione *S*-transferase (GST) fusions GST-YscM1 and GST-YscM2 immobilized on glutathione-Sepharose beads with different yersiniae lysates. To this end, *Y. enterocolitica* strain WA-314 (9), harboring the virulence plasmid pYV, and a plasmid-cured derivative (WA-C) were cultivated under conditions either permissive or restrictive for Yop expression and secretion (46). Beads were analyzed by denaturing gel electrophoresis (Fig. S1). We detected one band of ~95 kDa that was associated with GST-YscM1 and GST-YscM2 samples but not with GST alone. The appearance of this band did not depend on expression of the T3SS or the presence of the virulence plasmid, indicating a chromosomally encoded protein bound to YscM1 and YscM2. This protein was identified by mass spectrometry to be PEPC (data not shown).

To prove the relevance of this finding, we recombinantly expressed *Y. enterocolitica* PEPC in *Escherichia coli* and purified the protein to facilitate interaction studies. Subsequently, we performed native gel electrophoresis to test binding of recombinant PEPC to recombinant YscM1 and YscM2, respectively. Fig. 1*A* displays a Coomassie-stained native gel, demonstrating that GST-YscM1 causes a mobility shift of PEPC. PEPC mobility was also shifted in the presence of YscM1 released from GST (Fig. 1*B*). Electrophoretic mobility of PEPC was only slightly retarded when it was incubated with YscM2 prior to gel loading. Therefore, the native gel was electroblotted to verify the YscM2/PEPC interaction (Fig. 1*C*). The same blot was developed with anti-PEPC and anti-YscM2 sera successively. YscM2, when loaded alone, could not be detected, because YscM2 did not enter the gel under the conditions applied (38). This is due to the basic isoelectric point of YscM2 (9.79) and a pH of 7.4 of the native gel system. However, when a mixture of PEPC and YscM2 was applied on the gel, YscM2 co-localized with PEPC and could be detected after immunoblotting. Taken together, recombinant PEPC interacts with recombinant YscM1 and YscM2, respectively.

PEPC Activity Is Inhibited by YscM1 but Not by YscM2—PEPC catalyzes the carboxylation of phosphoenolpyruvate to form oxaloacetate in many microorganisms (45). This so-called anaplerotic reaction replenishes the tricarboxylic acid cycle intermediate oxaloacetate. Tricarboxylic acid cycle intermediates (oxaloacetate and α-ketoglutarate) are required for the biosynthesis of amino acids of the aspartate and glutamate families.

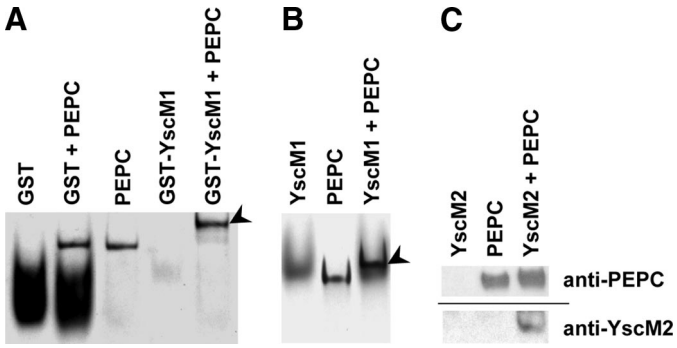

FIGURE 1. **Native gel electrophoresis reveals binding of PEPC to YscM1 and YscM2, respectively.** Recombinantly expressed and purified proteins were mixed, incubated at room temperature for 5 min, and loaded on 6% HEPES-buffered native polyacrylamide gels, as indicated. *A* and *B*, Coomassie-stained native gels; *C*, Western blot analysis after native gel electrophoresis. *A*, GST-YscM1 (dimeric) was in 2-fold excess over PEPC (tetrameric). The *arrowhead* indicates formation of GST-YscM1-PEPC complexes. The excess load of GST demonstrates that GST on its own exhibits no PEPC binding activity. *B*, YscM1-PEPC complex formation is indicated by an *arrowhead*. YscM1 (dimeric) was in 3-fold excess over PEPC (tetrameric). *C*, Western blot analysis of a native gel to demonstrate the YscM2/PEPC interaction. Following electroblotting, the same blot was developed with anti-PEPC and with anti-YscM2 sera successively. Data are representative of 3–5 independent experiments.

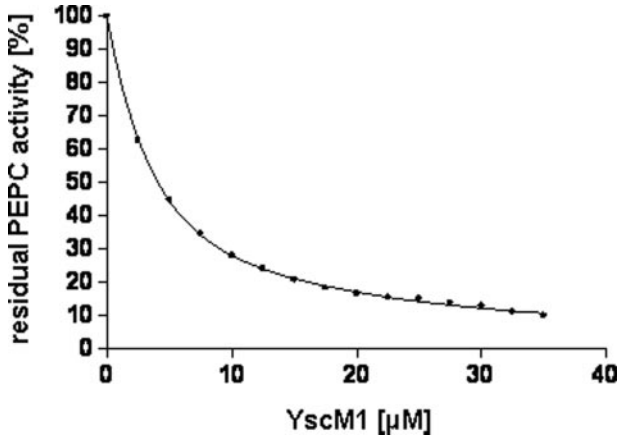

FIGURE 2. **Effect of YscM1 on PEPC activity.** PEPC activity was monitored spectrophotometrically by coupling the PEPC reaction with the malate dehydrogenase (*MDH*) reaction recording NADH oxidation at 340 nm. Relative PEPC activities $\Delta A_i/\Delta A_0$ in the presence of varying concentrations of YscM1 were plotted. All proteins were recombinantly expressed and purified to homogeneity. The inhibitory effect of YscM1 on PEPC activity was invariably demonstrated by four experimenters independently.

We analyzed the activity of PEPC in the presence of YscM1 or YscM2. PEPC enzymatic activity was determined by coupling the PEPC reaction to malate dehydrogenase and monitoring the rate of NADH oxidation spectrophotometrically at 340 nm (41). We observed a titratable inhibitory effect of YscM1 on PEPC activity (Fig. 2) and determined an IC_{50} value of 4 μM for YscM1. Determination of the K_i (1 μM) further revealed a competition between YscM1 and the substrate PEP (Fig. S2). By comparison, PEP analogues are described that inhibit homologous *E. coli* and plant PEPC with K_i values ranging from 18 to 85 μM (48–50), and allosteric inhibitors of PEPC, such as aspartate, inhibit PEPC in the millimolar range (51) (data not shown). To further evaluate the biological impact of the YscM1 inhibitory effect, we examined whether the PEPC inhibitor YscM1

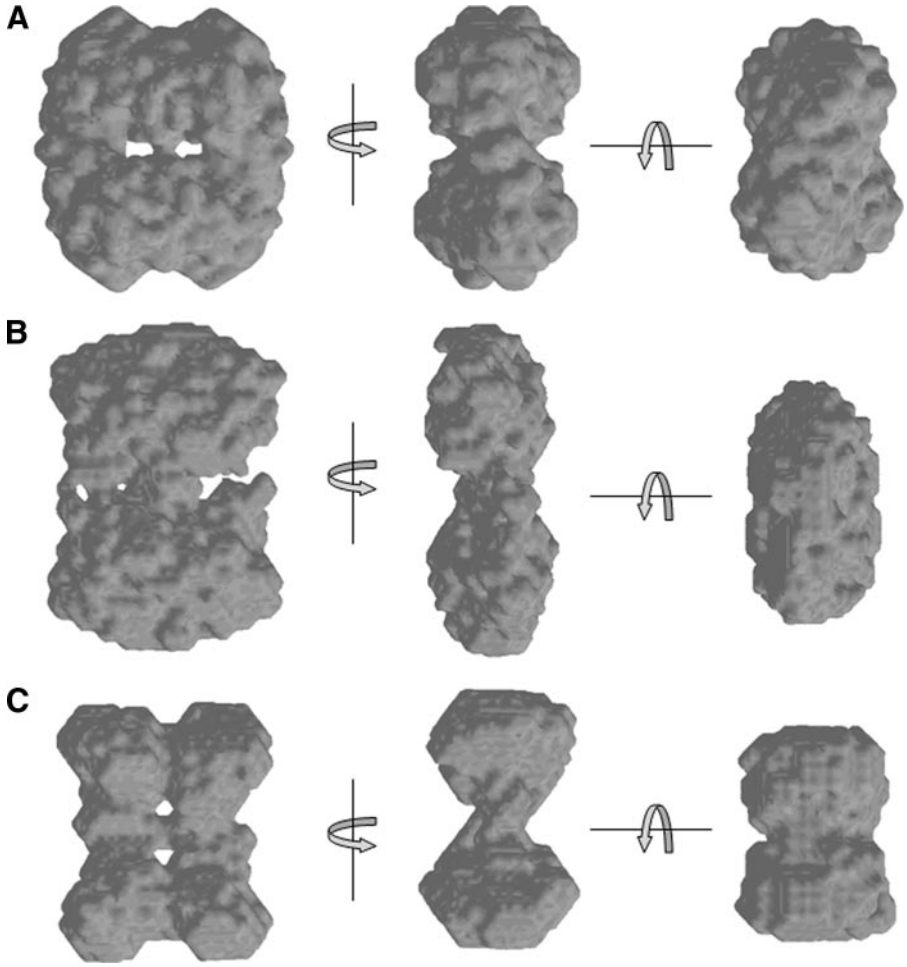

FIGURE 3. **Small angle x-ray scattering experiments reveal PEPC conformational changes mediated by YscM1 and YscM2, respectively.** Three views rotated 90°. *A*, low resolution model of the PEPC tetramer calculated from the scattering data assuming p22 symmetry. *B*, model calculated from the scattering data obtained from a YscM1/PEPC mixture. *C*, model calculated from the scattering data obtained from a YscM2/PEPC mixture. The scattering experiments were performed in duplicate with comparable results.

could antagonize acetyl-CoA, an allosteric activator of PEPC. In the presence of 50 μM acetyl-CoA, PEPC activity was stimulated by a factor of 2 relative to the PEPC control (100%), but only 10 μM of YscM1 was sufficient to fully compensate this stimulation (Fig. S3).

In contrast to YscM1, no significant influence of YscM2 on PEPC activity could be observed. Also, in the presence of YscM1, aspartate, or acetyl-CoA, we could not observe effects of YscM2 on PEPC activity (data not shown). In conclusion, our data suggest that YscM1 is a biologically relevant inhibitor of PEPC. Interestingly, although YscM2 clearly interacts with PEPC, we could not prove any significant influence of YscM2 on PEPC activity.

Small Angle X-ray Scattering Data Suggest That YscM1 and YscM2 Trigger Different Conformational Transitions of PEPC—Small angle x-ray scattering (SAXS) provides information about the overall shape of macromolecules in solution. Assuming that the interaction of YscM proteins with the allosteric enzyme PEPC could result in measurable conformational changes, we applied SAXS to study these interactions in solution. Fig. 3*A* shows three different views of the PEPC homotetramer calculated from the scattering data with the constraint of a p22 symmetry. This assumption is based on the results for the radius of gyration, molecular weight analysis, and *ab initio* shape reconstructions without any symmetry constraint. Further, this assumption is in line with the crystal structure of *E. coli* PEPC (52), which exhibits 80% identity with the *Yersinia* PEPC. This crystal structure shows that the homotetramer consists of two dimerized dimers, with the two dimers twisted relative to each other. The twist of the two dimers visible in the *E. coli* high resolution structure is also represented in our SAXS-based model of the *Yersinia* PEPC and is best illustrated in the *middle* and *right panels* of Fig. 3*A*. Fig. 3, *B* and *C*, shows the model of PEPC in the presence of YscM1 and in the presence of YscM2, respectively. YscM1 and YscM2 both cause dramatic conformational changes that are clearly distinct from one another. Similarly, however, YscM1 and YscM2 both induce conformational changes that reduce the twisting of the two dimers, leading to a more planar arrangement of the four subunits. These conformational changes may represent transitions from a relaxed "R" state to a tense "T" state, which are assumed to control the activity of allosteric enzymes. Due to the dramatic extent of the conformational changes induced by the YscM proteins and due to their small size relative to PEPC, it was not possible to draw any solid conclusion about the binding site of either YscM protein. Overall, the allosteric enzyme PEPC undergoes significant conformational transitions in the presence of either YscM1 or YscM2, further underscoring the biological relevance of these interactions. In particular, these data suggest that YscM2 could modulate PEPC activity under certain conditions that were not covered by our PEPC activity assay.

YscM1 Overproduction Causes Growth Restriction under Conditions Requiring PEPC—We reasoned that overproduction of YscM1 in *Y. enterocolitica* under conditions requiring PEPC activity should influence growth rates if YscM1 were to be an inhibitor of PEPC. It is known that in *E. coli*, PEPC is required when cells are grown on glucose as the sole carbon source (47, 53). Applying the Red recombinase technique (15), we generated a *Y. enterocolitica* mutant deleted of the PEPC-encoding gene *ppc*. The *ppc* mutant exhibited no significant proliferation on M9 minimal salts supplemented with 1% glucose, 0.01% casamino acids, and 10 μg/ml thiamine over a period of 7 h. By contrast, the parental strain and the *trans-*

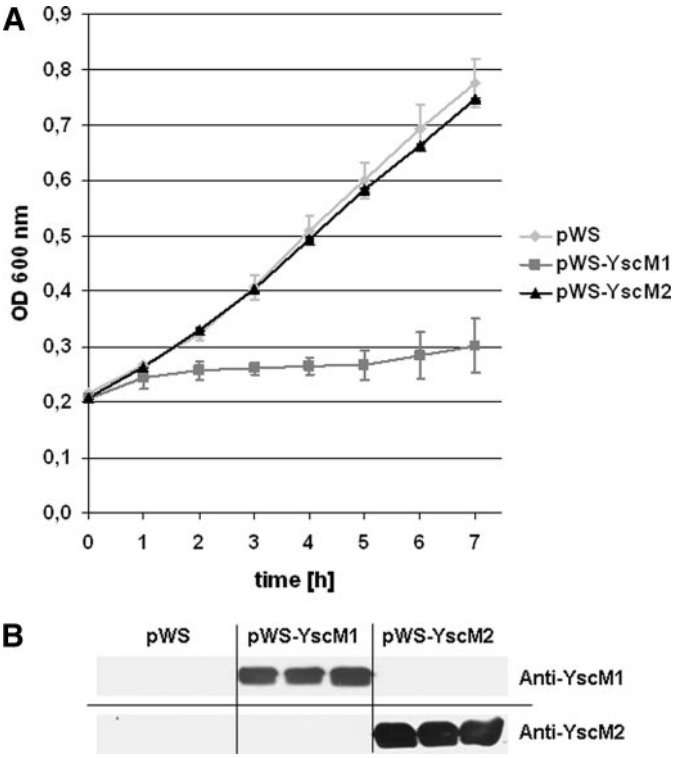

FIGURE 4. **Effect of YscM1/YscM2 overproduction on growth of *Y. enterocolitica* WA-314 under PEPC-requiring conditions at 27 °C.** Yersiniae harboring plasmids pWS-YscM1, pWS-YscM2, and pWS were grown in rich medium overnight. The next day, bacteria were resuspended in M9 minimal salts supplemented with 1% glucose, 0.01% casamino acids, and 10 μg/ml thiamine. 1 mM isopropyl β-D-thiogalactoside was added to all cultures at time 0 to induce overproduction of YscM1/YscM2 or as control (pWS). The optical density was determined at 600 nm (*A*), and bacteriostasis was checked by plating and colony counting. All experiments in triplicate from independent cultures (*error bars*, ± one S.D.). *B*, to control overproduction of YscM proteins, whole cell lysates from all cultures were loaded on denaturing SDS gels. After electroblotting, the membranes were developed with a serum raised against YscM1 or with a serum raised against YscM2, respectively. The experiment as represented here was repeated more than five times with similar results.

complemented *ppc* mutant grew well in the same medium, defining these conditions as PEPC-requiring (Fig. S4). The same conditions were chosen to dissect the effect of YscM1 and YscM2 overproduction on the growth rate of *Y. enterocolitica*. We constructed plasmids to overproduce YscM1 and YscM2 in yersiniae. *Y. enterocolitica* WA-314 was transformed with plasmid pWS-YscM1 or pWS-YscM2 or the control plasmid pWS and grown overnight in rich medium. The next day, bacteria were washed and resuspended in minimal medium composed as above and grown for several h at 27 °C, thus avoiding thermal stimulation of the T3SS regulon. Fig. 4*A* shows that yersiniae overproducing YscM1 were subjected to massive growth restriction, whereas overproduction of YscM2 had no significant effect on growth rates. Overproduction of YscM1 and YscM2 was confirmed by immunoblotting (Fig. 4*B*), and growth restriction was controlled by plating culture aliquots on solid media to determine colony forming units (data not shown). These results are in accordance with the *in vitro* analyses presented above and suggest that YscM1 also functions as an inhibitor of PEPC activity *in vivo*. As a further conclusion, the growth restriction mediated by YscM1 overproduction does not require the presence of additional components of the *Yersinia* T3SS, since growth was analyzed at 27 °C, which suppresses expression of the T3SS. In support of this conclusion, overproduction of YscM1 also repressed growth in *E. coli* BL21 (Fig. S5).

Mass Spectrometry Reveals that PEPC Reaction Affects Yop Biosynthesis—Assuming that YscM1 and possibly YscM2 manipulate amino acid biosynthesis pathways (particularly that of the aspartate family) via the PEPC reaction, the origin of amino acids incorporated into Yops should differ in the *ppc*, *yscM1*, and *yscM2* mutant strains compared with the wild type strain. To challenge this model, we cultured the strains in F-12 cell culture medium supplemented with 2% [U-$^{13}C_6$]glucose, induced Yop secretion by chelating calcium ions in the medium, and analyzed secreted Yops by MALDI-TOF mass spectrometry. The rationale for the choice of the medium was that it should contain sufficient amounts of amino acids to allow growth and T3 secretion of the *ppc* mutant but that it should be meager enough for the PEPC reaction to become limiting. This was indicated by slightly subdued growth of the *ppc* mutant in F-12 medium compared with the parental strain (data not shown). As expected, supplementation of the F-12 medium with [U-$^{13}C_6$]glucose led to a characteristic right shift and broadening of the mass spectra of YopE, YopH, and YopM proteins, which were secreted in large amounts and could be purified by SDS-PAGE (Fig. 5 and Figs. S6 and S7, compare *A* and *B*). The shift toward higher masses and the broadening in the mass patterns of a given fragment reflect that a fraction of amino acids used for Yop biosynthesis was made *de novo* using precursors derived from the proffered [U-$^{13}C_6$]glucose. However, the mass shift of less than 50 mass units also shows that the major fraction of Yop amino acids was still unlabeled and either synthesized from unlabeled precursors or recruited from unlabeled amino acids present in the medium.

As shown in Fig. 5*C*, the MS traces of ^{13}C-labeled YopM from the *ppc* mutant clearly differed from the corresponding signals of ^{13}C-labeled YopM from the parental strain grown under the same conditions. Specifically, a shift of the mass/charge ratios of peptide fragments toward lower values was observed. The same left shift was detected for YopH and YopE fragments from the *ppc* mutant (Figs. S6 and S7, compare *B* and *C*). We conclude that the PEPC reaction contributed to the biosynthesis of oxaloacetate-derived amino acids in the parental strain and that loss of this reaction in the *ppc* mutant was compensated by an increased uptake of unlabeled amino acids from the medium.

Using the same experimental approach, a possible influence of *yscM1* or *yscM2* deletion on PEPC activity and on Yop biosynthesis was analyzed. To rule out mutations in the chromosome of the *yscM1* and *yscM2* mutant strains, the mutated plasmids were transformed into the WA-C strain cured of its virulence plasmid. Transformants were subjected to the labeling experiment as described above, and secreted Yops were evaluated by mass spectrometry. The spectra of Yop peptides obtained from the *yscM1* and *yscM2* mutants were similar (Figs. 5, *D* and *E*, for YopM), but clearly differed from those of the parental strain (Fig. 5*B*) and the *ppc* mutant (Fig. 5*C*). Specifically, broadened mass patterns resembling the corresponding patterns in the spectra of the parental strain were observed.

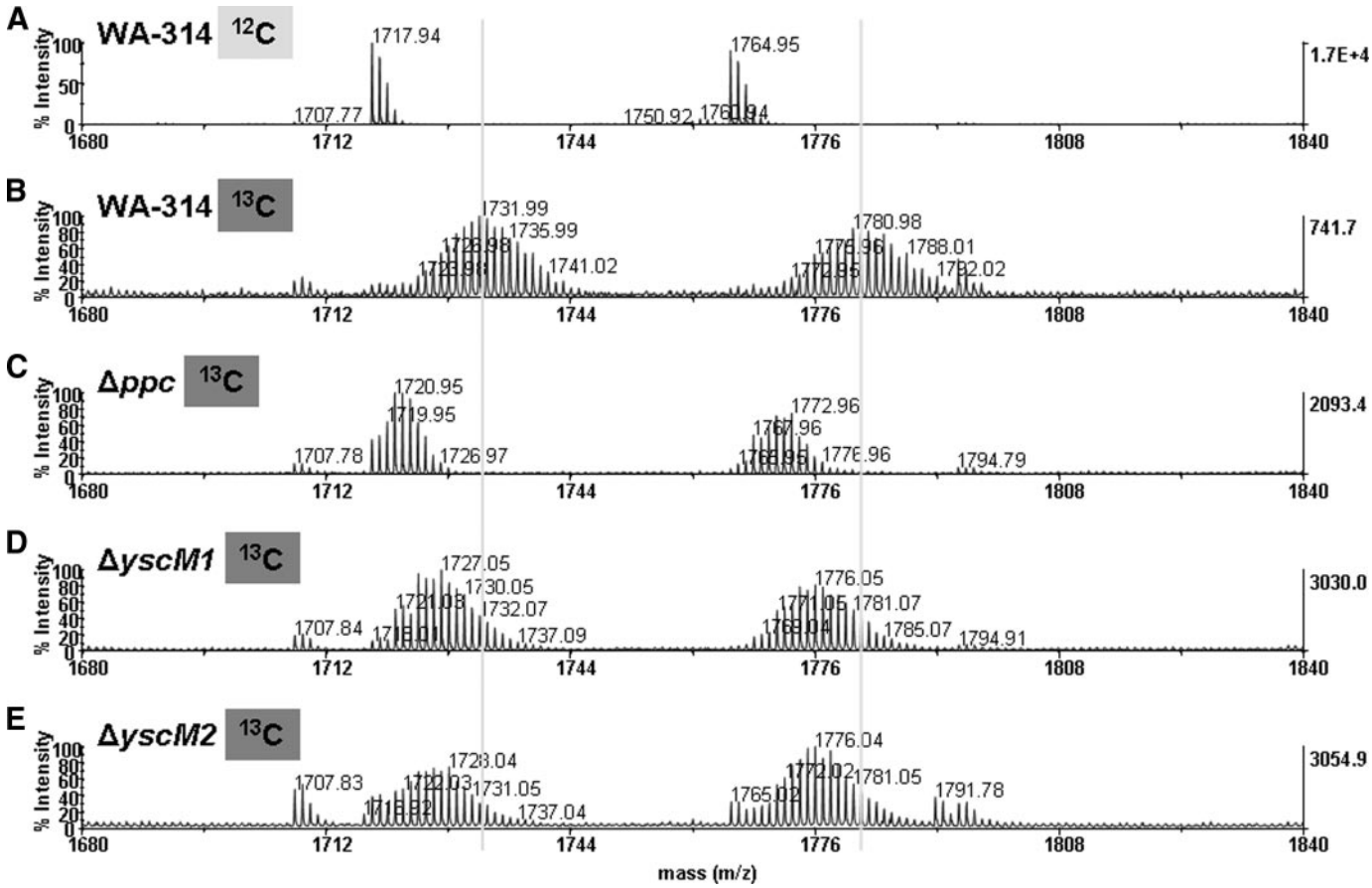

FIGURE 5. **MALDI-TOF mass spectrometry of peptide fragments derived from secreted YopM after feeding of yersiniae cultures with uniformly ^{13}C-labeled glucose.** *Y. enterocolitica* WA-314 and mutant strains *ppc*, *yscM1*, and *yscM2*, respectively, were grown in BHI medium overnight. The next day, bacteria were resuspended in F-12 medium supplemented with 0.2 mM $CaCl_2$ and 2% [U-$^{13}C_6$]glucose (^{13}C) or 2% unlabeled glucose (^{12}C). Cultures were incubated at 37 °C for 2 h, and then Yop secretion was induced, and cultivation was continued for 2 h at 37 °C. The supernatant of the cultures was collected, and proteins were precipitated by tricarboxylic acid and subjected to SDS-PAGE. The gel was Coomassie-stained, and the protein band corresponding to YopM was excised to perform MALDI-TOF mass spectrometry analysis. *A*, spectra of two YopM fragments from the parental strain WA-314 grown without labeling. *B*, spectra of the same two tryptic fragments of YopM when the strain was cultured in the presence of [U-$^{13}C_6$]glucose. *C–E*, corresponding spectra after [U-$^{13}C_6$]glucose labeling from the mutant strains as indicated. Corresponding analyses of YopE and YopH fragments are shown in Figs. S6 and S7. *Vertical light gray lines* were introduced to facilitate comparison of spectra. The data shown are representative of two independent experiments.

However, a small but significant shift toward lower masses indicated that both YscM1 and YscM2 influenced carbon fluxes from exogenous [U-$^{13}C_6$]glucose to amino acids used for Yop formation. The same conclusion could be drawn from observations in the MS spectra of YopE and YopH fragments (Figs. S6 and S7, compare *B–E*).

^{13}C Incorporation into Bacterial Amino Acids When [U-$^{13}C_6$]Glucose Was Provided during Yop Biosynthesis—In order to analyze the role of PEPC and YscM proteins in the synthesis of specific amino acids in cellular proteins, we used isotopologue profiling monitored by gas chromatography/mass spectrometry (43, 54). More specifically, *Y. enterocolitica* WA-314 and mutants thereof defective in PEPC, YscM1, or YscM2, respectively, were grown in F-12 cell culture medium containing 0.2% [U-$^{13}C_6$]glucose in a fermenter. After 2 h of growth, EGTA was added in analogy to the experiment designed for the MALDI-TOF analysis of Yop fragments. After 4 h, the bacteria were harvested in the late logarithmic state. Whole cell protein was hydrolyzed under acidic conditions, and the resulting amino acids were converted into *tert*-butyldimethylsilyl derivatives, which were subjected to GC/MS. The ^{13}C excess values of nine amino acids were determined from the mass ratios of selected ions (55). The data are summarized graphically in Fig. 6. The data are also shown numerically in Table S2.

In the experiment with the parental strain, the highest ^{13}C excess (2–3% ^{13}C) was found in Ala and Ser, followed by Asp, Gly, Ile, and Val (1–2%). Lower levels (0.6%) were observed in Phe. No incorporation was detected for Lys and Glu (<0.2%). The ^{13}C enrichments document that the transfer of label from the proffered ^{13}C-labeled glucose into the amino acids under study varied over a wide range under the experimental conditions. Probably, this is a consequence of the complex medium containing unlabeled amino acids (Table S1) that are incorporated into bacterial amino acids at different rates. With the exception of Lys and Glu, all amino acids under study acquired some label indicating that a fraction of Ala, Ser, Asp, Gly, Ile, Val, and Phe had been made *de novo* from exogenous [U-$^{13}C_6$]glucose.

In the experiment with the *ppc* mutant, Asp, Lys, and Glu were unlabeled (Fig. 6). The lack of ^{13}C enrichment of Asp is in sharp contrast to the experiment with the parental strain,

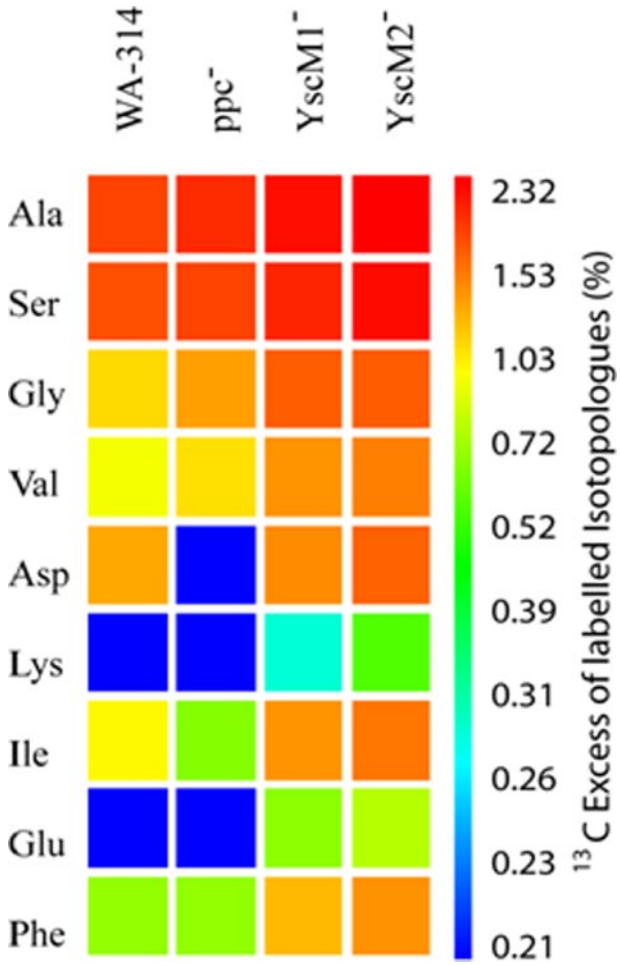

FIGURE 6. **Overall ^{13}C excess (mol %) of labeled isotopologues in amino acids derived from bacterial protein after feeding of yersiniae with 0.2% [U-$^{13}C_6$]glucose.** The *color map* indicates ^{13}C excess in quasilogarithmic form in order to visualize relatively small ^{13}C excess values. For each individual labeling experiment, samples were measured three times.

where significant ^{13}C label was detected in Asp. The ^{13}C excess in Ile from the *ppc* mutant was also lower than in Ile from the parental strain, whereas the values of the other amino acids under study were similar or even slightly higher than the corresponding values in amino acids from the parental strain. Obviously, the *de novo* biosynthesis of Asp using ^{13}C-labeled building blocks was stopped when the PEPC reaction was defective. Under these conditions, unlabeled Asp obtained from the culture medium appears to be used for protein biosynthesis. Moreover, the *de novo* biosynthesis of Ile was significantly reduced in the mutant, and a higher fraction of unlabeled Ile was taken from the medium. The fact that Asp but not Ala and Ser were unlabeled in the *ppc* mutant reveals that there is no detectable carbon flux to oxaloacetate and its downstream product Asp from ^{13}C-labeled C_3 metabolites (such as pyruvate and phosphoglycerate) serving as precursors for Ala and Ser. Similarly, no ^{13}C flux is observed into oxaloacetate/Asp via the citrate cycle using ^{13}C-labeled acetyl-CoA as a precursor (compare Figs. 8 and 9). Thus, the PEPC reaction is the predominant or even exclusive route leading to oxaloacetate and its downstream products under the experimental conditions.

In the experiment with mutants defective in the formation of YscM1 or YscM2, respectively, the ^{13}C excess values of all amino acids under study were similar (Fig. 6). This is in line with the results from the mass traces of Yop fragments (see above). In comparison with the labeling values observed in the experiments with the *ppc* mutant and the parental strain, all amino acids under study acquired more ^{13}C label. This also holds true for Asp and related amino acids where no or lower values were detected in the *ppc* mutant (see above). This modulation could reflect that some inhibitory effect of YscM1 or YscM2 on the PEPC reaction is lost with the deletion of YscM1 or YscM2, respectively; however, the increased *de novo* biosynthetic rates of many amino acids under study point to an additional and/or more general regulatory role of YscM1 and YscM2 on the central metabolic network.

More information was obtained by a detailed analysis of the isotopomer distributions in *tert*-butyldimethylsilyl-amino acids (for a detailed description of the method, see Refs. 43 and 44). Numerical values of ^{13}C excess of isotopomer groups are given in Table S3. The ratios of ^{13}C-labeled isotopomers carrying either two ($M + 2$) or three ($M + 3$) ^{13}C atoms in Ala, Asp, Ser, and Phe from the parental strain and the mutants are displayed in Fig. 7.

Within the limits of experimental accuracy, the ratios were identical in amino acids from YscM1 and YscM2 mutants, respectively. Again, this indicates that YscM1 and YscM2 serve similar roles in the modulation of the metabolism. In all experiments, Ser was characterized by the ($M + 3$) isotopologue (Fig. 7*C*), which can be explained by conversion of [U-$^{13}C_6$]glucose into [U-$^{13}C_3$]Ser via [U-$^{13}C_3$]triose phosphate and [U-$^{13}C_3$]phosphoglycerate, which can be formed by reactions of glycolysis (Fig. 8) and/or the Entner-Doudoroff pathway. Indeed, all genes required for these pathways have been identified in *Y. enterocolitica* (56) (KEGG data base). The fact that ($M + 2$)-Ser is apparently absent shows that the alternative pathway of Ser formation (*i.e.* hydroxymethylation of [U-$^{13}C_2$]Gly) did not contribute to Ser biosynthesis. As shown in Fig. 7*C*, the isotopomer profile of Ser was very similar in the parental strain and all mutants under study. This suggests that the isotopomer distribution was also similar in the Ser precursors, such as triose phosphate and phosphoglycerate, and it can be concluded that carbon flux from the labeled glucose precursor to triose phosphate and phosphoglycerate was not affected by deletion of PEPC, YscM1, or YscM2, respectively (compare Figs. 8–10).

The isotopomer distribution of Phe reflects the composition of the precursors, phosphoenol pyruvate and erythrose 4-phosphate, via the shikimate pathway. As shown in Fig. 7*D*, ($M + 3$)- and ($M + 2$)-isotopomer groups were present in Phe from all experiments. Notably, the abundances of both isotopomer groups were higher in Phe from YscM1 and YscM2 mutants. Since the labeling pattern of Ser suggested similar patterns in phosphoglycerate and its downstream product, phosphoenol pyruvate, it can be inferred that the increased abundances must be due to differences in the erythrose 4-phosphate precursor. On this basis, deletion of YscM1 and YscM2 appears to increase carbon flux from the proffered glucose into the tetrose phos-

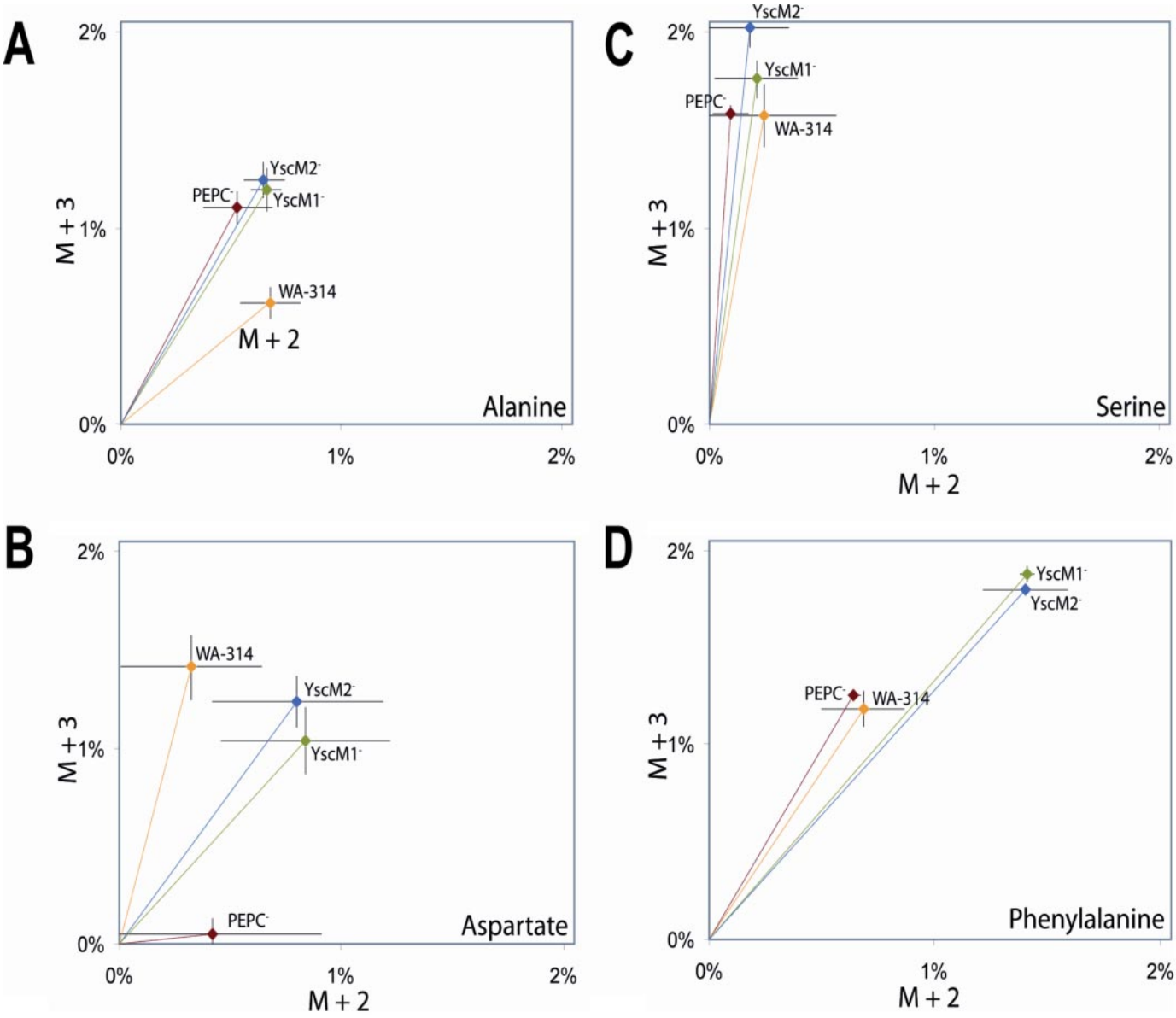

FIGURE 7. **Isotopologue excess (mol %) of biosynthetic Ala (*A*), Asp (*B*), Ser (*C*), and Phe (*D*) derived from bacterial protein after feeding of yersiniae with 0.2% [U-$^{13}C_6$]glucose.** The *colors* indicate different strains. Each sample was measured three times. ($M + 3$) or ($M + 2$), molecule with three or two ^{13}C atoms, respectively.

phate via the nonoxidative branch of the pentose phosphate pathway (Fig. 10).

The isotopomer compositions of Ala were characterized by ($M + 3$) and ($M + 2$) species at similar abundances (Fig. 7*A*). Ala from the *ppc* mutant showed a similar if not identical ($M + 3$)/($M + 2$) ratio as in Ala from the YscM mutants. On the other hand, Ala from the parental strain had a different ratio with a lower value for the ($M + 3$)-isotopologue (Fig. 7*A*). The data document that a significant fraction of Ala was derived via [U-$^{13}C_3$]PEP and [U-$^{13}C_3$]pyruvate, giving rise to the ($M + 3$)-isotopologue. Again, the formation of [U-$^{13}C_3$]pyruvate from proffered [U-$^{13}C_6$]glucose can be explained by glycolysis or the Entner-Doudoroff pathway. The doubly labeled isotopomer group characterized by ($M + 2$)-Ala had a more complex biosynthetic history, where pyruvate must have been assembled from a $^{13}C_2$ fragment and a $^{12}C_1$ fragment. This process can be explained by the action of malic enzyme (Fig. 8). The fact that ($M + 3$) and ($M + 2$) species can be detected in Ala from all experiments indicates that all of these processes are operative in the parental strain as well as in the mutants. However, the different ratios (Fig. 7*A*) demonstrate that the efficiencies of the processes are modulated by the mutations. More specifically, the higher ($M + 3$) values in the PEPC mutants and especially in the YscM mutants document that more carbon from glucose is transferred to pyruvate and alanine, respectively, via the direct pathways by glycolysis and/or the Entner-Doudoroff pathway (Figs. 9 and 10).

The distribution of ($M + 3$)- and ($M + 2$)-isotopomers was also different in Asp from the various experiments (Fig. 7*B*). Since Asp is derived from oxaloacetate by transamination, the ($M + 3$)-isotopologue can be considered as a marker for the PEPC reaction, where a $^{13}C_3$-labeled phosphoenol pyruvate

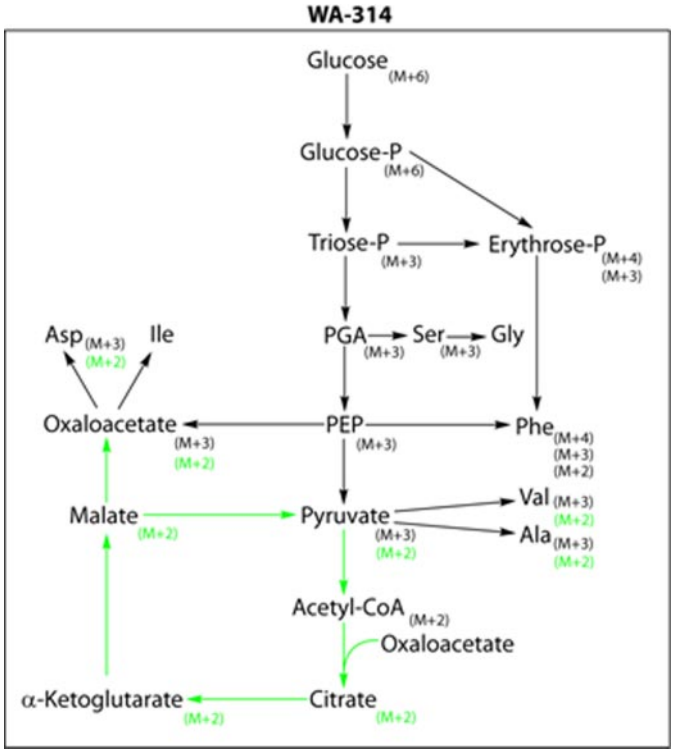

FIGURE 8. **Reaction network of the central carbon metabolism in *Y. enterocolitica* WA-314 The model is based on labeling experiments with [U-$^{13}C_6$]glucose and isotopologue profiling of protein-derived amino acids.** ($M + 6$), ($M + 4$), ($M + 3$), and ($M + 2$) subscripts indicate isotopologues containing six, four, three, or two ^{13}C atoms in excess, respectively. *Green arrows* and *green subscripts* indicate isotopologues due to reactions in the citrate cycle and the malic enzyme. *PGA*, 3-phosphoglycerate.

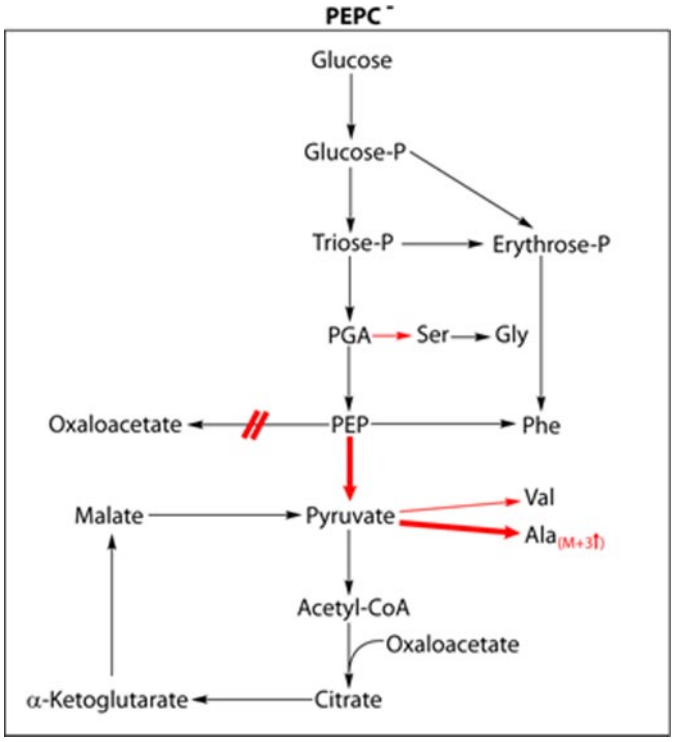

FIGURE 9. **Reaction network of the central carbon metabolism in *Y. enterocolitica* PEPC⁻.** *Red arrows* indicate increased flux conducive of the isotopologues shown as *red subscripts*. For more details, see the legend to Fig. 8.

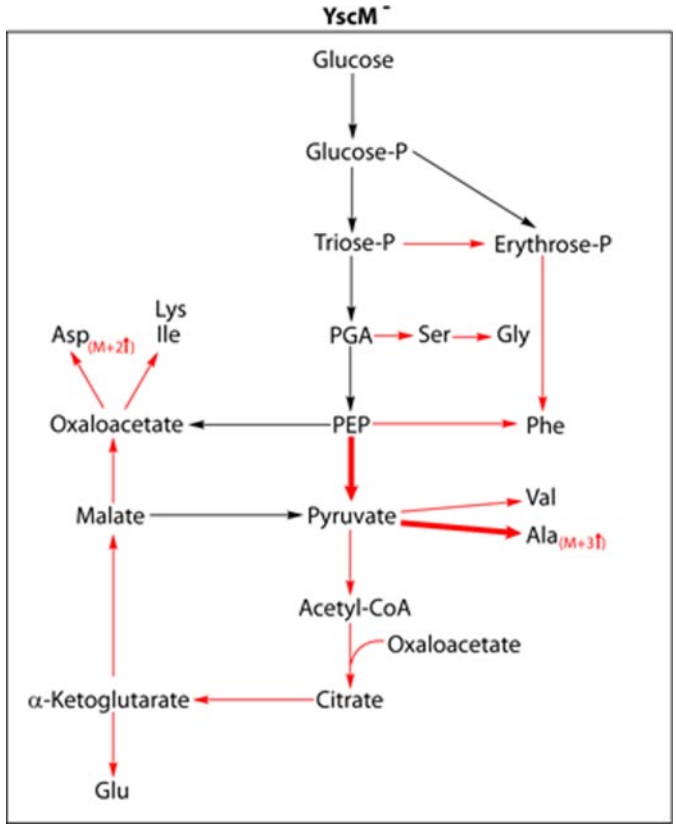

FIGURE 10. **Reaction network of the central carbon metabolism in *Y. enterocolitica* YscM1⁻ or YscM2⁻.** For more details, see the legend to Fig. 9.

and unlabeled CO_2 are converted into [$^{13}C_3$]oxaloacetate. Since, on the basis of the Ser profile, phosphoenol pyruvate appeared to comprise only ($M + 3$) species at significant amounts, the presence of ($M + 2$)-isotopologues does not reflect the PEPC reaction but rather indicates formation of oxaloacetate by the citrate cycle, where $^{13}C_2$-labeled acetyl-CoA (derived from [$^{13}C_3$]pyruvate by pyruvate dehydrogenase) is introduced (Fig. 8). As shown in Fig. 7*B*, the YscM1 and YscM2 mutants were characterized by higher values for the ($M + 2$)-isotopomer groups, indicating that flux via the citrate cycle was increased by deletion of either YscM1 or YscM2 (Fig. 10). On the other hand, the abundances of the ($M + 3$)-isotopologues appeared to be lower in the mutants (Fig. 7*B*), suggesting that carbon flux via the PEPC reaction was slightly lower under the deficiency of YscM1 or YscM2, respectively.

Taken together, isotopologue profiling confirmed that the PEPC reaction contributed to amino acid biosynthesis under conditions of Yop secretion and that *yscM1* and *yscM2* were involved in control of carbon fluxes through the central metabolic network of *Y. enterocolitica*. In contrast to the *in vitro* studies with recombinant YscM proteins, *yscM1* and *yscM2* mutants exhibited very similar isotopologue profiles.

DISCUSSION

Bifunctionality of the YscM Proteins—The *Yersinia* T3SS components YscM1/LcrQ and YscM2 are involved in regulation of Yop expression (18–20, 23). This regulatory function is mediated in concert with YopD, LcrH, and SycH (19, 26, 28). Stainer *et al.* (19) described the phenomenon that deletion of

either *yscM1* or *yscM2* alone had no influence on the level of Yop expression and secretion, whereas the *yscM1*/*yscM2* double mutant exhibited the *lcrQ* phenotype known from *Y. pestis* and *Y. pseudotuberculosis*. Consequently, a functional redundancy of the YscM proteins was assumed. In addition to this described function, we show here that YscM1 and YscM2 interact with the metabolic enzyme PEPC. The interaction of YscM1 and YscM2 with PEPC has been demonstrated unequivocally by applying affinity purification, native gel electrophoresis, and SAXS experiments. The influence of YscM1 on PEPC activity is of inhibitory nature as revealed by PEPC activity assays and overproduction experiments. The role of YscM2 remains elusive, since we were unable to attribute any influence of YscM2 on PEPC activity *in vitro*. Further, its overproduction had no effect on growth of yersiniae under conditions requiring PEPC activity. In marked contrast, mass spectrometry following stable isotope labeling revealed an influence of *yscM2* deletion on biosynthesis of Yops similar to that associated with the *yscM1* deletion, and, more specifically, isotopologue profiling revealed similarly increased carbon flux from glucose into amino acid for both *yscM* deletion strains. This discrepancy could be attributed to an additional component, proteinaceous or low molecular weight compound, required for YscM2 to modulate PEPC activity that is missing in our *in vitro* assays and under the conditions chosen for YscM2 overexpression.

Taken together, with respect to this newly discovered function, YscM1 and YscM2 do not display complete redundancy. From a Darwinian point of view, this is as expected, since a functional equivalence of the YscM proteins cannot explain their stable coexistence. The acquisition of a second copy of the *yscM* gene in *Y. enterocolitica* points to a more sophisticated regulation of metabolism in this species compared with *Y. pestis* and *Y. pseudotuberculosis*, which harbor only the *yscM1* orthologue *lcrQ*.

The YscM1/PEPC Interaction, a Case of Molecular Co-adaptation?—It is worthwhile to mentioning that we have determined the K_m (or more precisely, the $S_{0,5}$ value) for the substrate PEP to be 4.1 mM for *Y. enterocolitica* PEPC, whereas the reported $K_m/S_{0,5}$ (PEP) values for the 80% identical *E. coli* PEPC range from 0.1 to 0.2 mM (51, 52). Since we found that YscM1 competes for the PEP binding site, the unexpectedly high $S_{0,5}$ (PEP) may indicate that *Yersinia* PEPC has evolutionarily co-adapted to the interaction with YscM1/LcrQ. This hypothesis might be revisable; *Y. enterocolitica* biotype 1A does not harbor the virulence plasmid pYV, which encodes the T3SS. Given that the biotype 1A lineage diverged from the *Yersinia* lineage either before acquisition of the virulence plasmid or early after its acquisition, the catalytic properties of *Yersinia* biotype 1A PEPC and its response to YscM1/LcrQ interaction should differ from that of PEPC of pYV-carrying yersiniae. Moreover, if this molecular co-adaptation hypothesis holds, changed PEPC properties may have triggered further adaptation processes, resulting in divergence of the metabolism of T3SS-harboring yersiniae compared with biotype 1A strains. This scenario might also explain why the phenotypes of the *yscM* deletion mutants, although clearly linking T3S to metabolism, are not as clear cut as expected.

Cross-talk between T3SS and Metabolism—It was outlined above that assembly and operation of the T3SS are metabolically demanding. It therefore seems plausible that functional T3 secretion requires a coordinated adaptation of metabolic pathways. Here, we propose that modulation of *Yersinia* PEPC activity could be necessary to adapt to different metabolic requirements during infection. During those stages of infection relying on T3SS activity, two principle situations might be distinguishable. One phase is characterized by the massive synthesis of Yops and other T3SS components in preparation of phagocytic attack ("loading"). Under these conditions, the provision of building blocks for amino acid synthesis should require an active PEPC enzyme to replenish the tricarboxylic acid cycle. The second phase is initiated by contact with phagocytic cells and requires the rapid injection of the presynthesized pool of Yops ("shooting"). The latter conditions might force yersiniae to prioritize maintenance of energy charge over biosynthetic processes and propagation. Shutdown of anaplerosis via inhibition of PEPC could push the balance in that direction. After injection of the presynthesized Yop pool, biosynthesis of new Yops should be prioritized again and so on. This "load-and-shoot cycle" model states that functioning of the T3SS *in vivo* requires a reprogramming of metabolic pathways and that it is the bifunctionality of YscM/LcrQ that allows coordination of Yop expression and metabolism. YscM/LcrQ interact with a multitude of T3SS proteins, mostly T3SS chaperones, which prompted us to speculate that YscM/LcrQ proteins function as a molecular interface that senses if T3SS chaperones are loaded with Yops and transduces this information into repression or derepression of Yop synthesis in concert with YopD, LcrH, and SycH (14, 31). In parallel, this integrated information is also ideally suited to coordinate the metabolism via modulation of PEPC activity and possibly other metabolic enzymes.

The YscM1/PEPC Interaction, a Missing Link to Low Calcium Response?—It has long been known that virulence of *Y. pestis* is lost upon cultivation at 37 °C and that avirulent variants are rapidly enriched. It was found that virulence could be maintained by the addition of calcium ions (6), glutamate, aspartate, or bicarbonate (57). This prompted Baugh *et al.* (58) to compare carbon dioxide fixation into oxaloacetate in virulent and avirulent *Y. pestis*. However, they were unable to demonstrate any difference between virulent and avirulent strains. Later, Fowler and Brubaker (59) emphasized the importance of CO_2 fixation into oxaloacetate for *Y. pestis*, especially in the context of the lack of aspartase activity in this species (60). In contrast, degradation of L-aspartate via aspartase, fumarase, and malic dehydrogenase enables the regeneration of oxaloacetate in *Y. pseudotuberculosis* (60). Recently, Lee *et al.* (61) could demonstrate that T3 secretion in *Yersinia* is activated by glutamate, glutamine, aspartate, and asparagine. Although these pioneering studies pointed at an interrelationship between virulence and metabolism in *Yersinia*, particularly emphasizing the PEPC reaction, such a conjunction has never been demonstrated on a molecular level. An inhibitory effect of LcrQ on PEPC activity fits with these previous observations of restricted growth in *Y. pestis*. However, the *lcrQ* mutant is characterized by growth restriction at 37 °C in the presence of Ca^{2+} ions, which means that, provided that PEPC is crucially involved in growth cessa-

tion of *Y. pestis*, another factor takes over inhibition of PEPC in the absence of LcrQ. YopH could be such a candidate, since the first 128 amino acids of YopH show 42% identity to LcrQ (23).

Perspectives—The YscM/LcrQ proteins interact with several components of the T3SS and represent major nodal points of the T3SS regulatory network (14, 31). A complete T3SS interactome is therefore required to elucidate the significance of the PEPC/YscM interactions. The lack of understanding of the YscM2/PEPC interaction might be due to cooperative interaction partners that are missing under the conditions tested. Also, the gap in our understanding of growth restriction in the absence of LcrQ, as discussed above, might be bridged by increasing knowledge of more protein/protein interactions. SAXS experiments have been proven to be a powerful tool to analyze PEPC/YscM interactions in solution. In continuation, we will compare the conformational transitions of PEPC caused by YscM1 and YscM2 with those induced by known allosteric effectors to add to the understanding of the mode of action.

We have demonstrated here that the introduction of ^{13}C labeling via [U-$^{13}C_6$]glucose, followed by MALDI-TOF and GC/MS analysis, respectively, enables to distinguish the *ppc*, *yscM1*, and *yscM2* mutants from the parental strain with respect to Yop synthesis and amino acid biosynthesis. GC/MS-based analysis of ^{13}C enrichment and isotopologue patterns indicates that next to a modulation of the PEPC reaction, flux through the central metabolic network, including the citrate cycle and the pentose phosphate pathway, appears to be triggered by YscM, but more sophisticated methods, such as NMR-based isotopologue profiling (62), will be required to gain quantitative insights into the positional redistribution of carbon fluxes caused by the deletions. In addition, a more direct approach to monitor the contribution of carbon dioxide fixation by PEPC would be to introduce ^{13}C labeling via bicarbonate. Time-resolved metabolic profiling will be required to challenge the load-and-shoot cycle model.

Y. enterocolitica strains deleted of *yscM1*, *yscM2*, and *ppc*, respectively, have to be further characterized in cell culture and mouse infection models to shed light on the cross-talk between T3SS and metabolism in its biological context. Another step will be the characterization of the temperature-sensitive *yscM1*/*yscM2* double mutant and the *lcrQ* mutants of *Y. pseudotuberculosis* and *Y. pestis*. The interpretation of these data, however, will be more complicated because of the bifunctionality of the YscM/LcrQ proteins. Since the *yscM* genes are redundant with respect to their Yop regulatory function (19), deletions of either *yscM1* or *yscM2* alone are ideally suited to study the PEPC regulatory effect without disturbing the Yop regulatory network.

Further, deletion of *ppc* in *Y. pseudotuberculosis* and *Y. pestis* is expected to have more dramatic effects on T3 secretion, since the LCR-related growth restriction of both species is more pronounced compared with *Y. enterocolitica* (7). Provided that PEPC is the key enzyme involved in growth arrest of *Y. pestis*, it should be an ideal candidate for drug targeting.

Acknowledgments—We acknowledge the excellent assistance of Gabriele Liegl and Emilia Sieger.

REFERENCES

1. Troisfontaines, P., and Cornelis, G. R. (2005) *Physiol.* (*Bethesda*) **20,** 326–339
2. Heesemann, J., Sing, A., and Trülzsch, K. (2006) *Curr. Opin. Microbiol.* **9,** 55–61
3. Marketon, M. M., DePaolo, R. W., DeBord, K. L., Jabri, B., and Schneewind, O. (2005) *Science* **309,** 1739–1741
4. Rosqvist, R., Magnusson, K. E., and Wolf-Watz, H. (1994) *EMBO J.* **13,** 964–972
5. Cornelis, G. R., Boland, A., Boyd, A. P., Geuijen, C., Iriarte, M., Neyt, C., Sory, M. P., and Stainier, I. (1998) *Microbiol. Mol. Biol. Rev.* **62,** 1315–1352
6. Higuchi, K., Kupferberg, L. L., and Smith, J. L. (1959) *J. Bacteriol.* **77,** 317–321
7. Carter, P. B., Zahorchak, R. J., and Brubaker, R. R. (1980) *Infect. Immun.* **28,** 638–640
8. Goguen, J. D., Yother, J., and Straley, S. C. (1984) *J. Bacteriol.* **160,** 842–848
9. Heesemann, J., Algermissen, B., and Laufs, R. (1984) *Infect. Immun.* **46,** 105–110
10. Ramamurthi, K. S., and Schneewind, O. (2002) *Annu. Rev. Cell Dev. Biol.* **18,** 107–133
11. Woestyn, S., Allaoui, A., Wattiau, P., and Cornelis, G. R. (1994) *J. Bacteriol.* **176,** 1561–1569
12. Wilharm, G., Lehmann, V., Neumayer, W., Trček, J., and Heesemann, J. (2004) *BMC Microbiol.* **4,** 27
13. Akeda, Y., and Galan, J. E. (2005) *Nature* **437,** 911–915
14. Wilharm, G., Dittmann, S., Schmid, A., and Heesemann, J. (2007) *Int. J. Med. Microbiol.* **297,** 27–36
15. Wilharm, G., Lehmann, V., Krauss, K., Lehnert, B., Richter, S., Ruckdeschel, K., Heesemann, J., and Trülzsch, K. (2004) *Infect. Immun.* **72,** 4004–4009
16. Brubaker, R. R. (2005) *Infect. Immun.* **73,** 4743–4752
17. Wiley, D. J., Rosqvist, R., and Schesser, K. (2007) *J. Mol. Biol.* **373,** 27–37
18. Pettersson, J., Nordfelth, R., Dubinina, E., Bergman, T., Gustafsson, M., Magnusson, K. E., and Wolf-Watz, H. (1996) *Science* **273,** 1231–1233
19. Stainier, I., Iriarte, M., and Cornelis, G. R. (1997) *Mol. Microbiol.* **26,** 833–843
20. Cambronne, E. D., Cheng, L. W., and Schneewind, O. (2000) *Mol. Microbiol.* **37,** 263–273
21. Cambronne, E. D., Sorg, J. A., and Schneewind, O. (2004) *J. Bacteriol.* **186,** 829–841
22. Allaoui, A., Schulte, R., and Cornelis, G. R. (1995) *Mol. Microbiol.* **18,** 343–355
23. Rimpilainen, M., Forsberg, A., and Wolf-Watz, H. (1992) *J. Bacteriol.* **174,** 3355–3363
24. Michiels, T., Vanooteghem, J. C., Lambert de Rouvroit, C., China, B., Gustin, A., Boudry, P., and Cornelis, G. R. (1991) *J. Bacteriol.* **173,** 4994–5009
25. Wattiau, P., Bernier, B., Deslee, P., Michiels, T., and Cornelis, G. R. (1994) *Proc. Natl. Acad. Sci. U. S. A.* **91,** 10493–10497
26. Williams, A. W., and Straley, S. C. (1998) *J. Bacteriol.* **180,** 350–358
27. Wulff-Strobel, C. R., Williams, A. W., and Straley, S. C. (2002) *Mol. Microbiol.* **43,** 411–423
28. Cambronne, E. D., and Schneewind, O. (2002) *J. Bacteriol.* **184,** 5880–5893
29. Swietnicki, W., O'Brien, S., Holman, K., Cherry, S., Brueggemann, E., Tropea, J. E., Hines, H. B., Waugh, D. S., and Ulrich, R. G. (2004) *J. Biol. Chem.* **279,** 38693–38700
30. Schmid, A., Dittmann, S., Grimminger, V., Walter, S., Heesemann, J., and Wilharm, G. (2006) *Protein Expression Purif.* **49,** 176–182
31. Dittmann, S., Schmid, A., Richter, S., Trulzsch, K., Heesemann, J., and Wilharm, G. (2007) *BMC Microbiol.* **7,** 67
32. Dacheux, D., Epaulard, O., de Groot, A., Guery, B., Leberre, R., Attree, I., Polack, B., and Toussaint, B. (2002) *Infect. Immun.* **70,** 3973–3977
33. Kim, W., and Surette, M. G. (2004) *Mol. Microbiol.* **54,** 702–714
34. Rietsch, A., Wolfgang, M. C., and Mekalanos, J. J. (2004) *Infect. Immun.* **72,** 1383–1390
35. Wang, Q., Frye, J. G., McClelland, M., and Harshey, R. M. (2004) *Mol. Microbiol.* **52,** 169–187

36. Rietsch, A., and Mekalanos, J. J. (2006) *Mol. Microbiol.* **59,** 807–820
37. Locher, M., Lehnert, B., Krauss, K., Heesemann, J., Groll, M., and Wilharm, G. (2005) *J. Biol. Chem.* **280,** 31149–31155
38. Wilharm, G., Neumayer, W., and Heesemann, J. (2003) *Protein Expression Purif.* **31,** 167–172
39. Schlee, M., Krug, T., Gires, O., Zeidler, R., Hammerschmidt, W., Mailhammer, R., Laux, G., Sauer, G., Lovric, J., and Bornkamm, G. W. (2004) *J. Virol.* **78,** 3941–3952
40. Aepfelbacher, M., Trasak, C., Wilharm, G., Wiedemann, A., Trülzsch, K., Krauss, K., Gierschik, P., and Heesemann, J. (2003) *J. Biol. Chem.* **278,** 33217–33223
41. Smith, T. E. (1968) *Arch. Biochem. Biophys.* **128,** 611–622
42. Trülzsch, K., Sporleder, T., Igwe, E. I., Rüssmann, H., and Heesemann, J. (2004) *Infect. Immun.* **72,** 5227–5234
43. Eylert, E., Schär, J., Mertins, S., Stoll, R., Bacher, A., Goebel, W., and Eisenreich, W. (2008) *Mol. Microbiol.* **69,** 1008–1017
44. Lee, W. N., Byerley, L. O., Bergner, E. A., and Edmond, J. (1991) *Biol. Mass. Spectrom.* **20,** 451–458
45. Roessle, M. W., Klaering, R., Ristau, U., Robrahn, B., Jahn, D., Gehrmann, T., Konarev, P., Round, A., Fiedler, S., Hermes, C., and Svergun, D. (2007) *J. Appl. Crystallogr.* **4,** s190–s194
46. Heesemann, J., Gross, U., Schmidt, N., and Laufs, R. (1986) *Infect. Immun.* **54,** 561–567
47. Sauer, U., and Eikmanns, B. J. (2005) *FEMS Microbiol. Rev.* **29,** 765–794
48. Izui, K., Matsuda, Y., Kameshita, I., Katsuki, H., and Woods, A. E. (1983) *J. Biochem.* (*Tokyo*) **94,** 1789–1795
49. García-Alles, L. F., and Erni, B. (2002) *Eur. J. Biochem.* **269,** 3226–3236
50. Kai, Y., Matsumura, H., and Izui, K. (2003) *Arch. Biochem. Biophys.* **414,** 170–179
51. Terada, K., Murata, T., and Izui, K. (1991) *J. Biochem.* (*Tokyo*) **109,** 49–54
52. Kai, Y., Matsumura, H., Inoue, T., Terada, K., Nagara, Y., Yoshinaga, T., Kihara, A., Tsumura, K., and Izui, K. (1999) *Proc. Natl. Acad. Sci. U. S. A.* **96,** 823–828
53. Eiteman, M. A., and Altman, E. (2006) *Trends Biotechnol.* **24,** 530–536
54. Fischer, E., and Sauer, U. (2003) *Eur. J. Biochem.* **270,** 880–891
55. Antoniewicz, M. R., Kelleher, J. K., and Stephanopoulos, G. (2007) *Anal. Chem.* **79,** 7554–7559
56. Thomson, N. R., Howard, S., Wren. B. W., Holden, M. T., Crossman, L., Challis, G. L., Churcher, C., Mungall, K., Brooks, K., Chillingworth, T., Feltwell, T., Abdellah, Z., Hauser, H., Jagels, K., Maddison, M., Moule, S., Sanders, M., Whitehead, S., Quail, M. A., Dougan, G., Parkhill, J., and Prentice, M. B. (2006) *PLoS Genet.* **2,** e206
57. Delwiche, E. A., Fukui, G. M., Andrews, A. W., and Surgalla, M. J. (1959) *J. Bacteriol.* **77,** 355–360
58. Baugh, C. L., Lanham, J. W., and Surgalla, M. J. (1964) *J. Bacteriol.* **88,** 553–558
59. Fowler, J. M., and Brubaker, R. R. (1994) *Infect. Immun.* **62,** 5234–5241
60. Dreyfus, L. A., and Brubaker, R. R. (1978) *J. Bacteriol.* **136,** 757–764
61. Lee, V. T., Mazmanian, S. K., and Schneewind, O. (2001) *J. Bacteriol.* **183,** 4970–4978
62. Eisenreich, W., Slaghuis, J., Laupitz, R., Bussemer, J., Stritzker, J., Schwarz, C., Schwarz, R., Dandekar, T., Goebel, W., and Bacher, A. (2006) *Proc. Natl. Acad. Sci. U. S. A.* **103,** 2040–2045

Cross-talk between Type Three Secretion System and Metabolism in *Yersinia*

Annika Schmid, Wibke Neumayer, Konrad Trülzsch, Lars Israel, Axel Imhof, Manfred Roessle, Guido Sauer, Susanna Richter, Susan Lauw, Eva Eylert, Wolfgang Eisenreich, Jürgen Heesemann and Gottfried Wilharm

J. Biol. Chem. 2009, 284:12165-12177.
doi: 10.1074/jbc.M900773200 originally published online February 25, 2009
